Notes on Histotomography

Lionheart, William R.B.

2018

MIMS EPrint: **2018.8**

Manchester Institute for Mathematical Sciences
School of Mathematics

The University of Manchester

Reports available from: http://eprints.maths.manchester.ac.uk/
And by contacting: The MIMS Secretary
School of Mathematics
The University of Manchester
Manchester, M13 9PL, UK

ISSN 1749-9097

Notes on Histotomography

W.R.B Lionheart

March 8, 2018

Abstract

In many tomographic imaging problems the data consists of integrals along lines or curves. Increasingly we are seeing "rich tomography" problems where the quantity imaged is higher dimensional than a scalar per voxel, including vectors tensors and functions. The data can also be higher dimensional and in many cases consists of a one or two dimensional spectrum for each ray. In many such cases the data contains not just integrals along rays but the distribution of values along the ray. If this is discretized into bins we can think of this as a histogram. In this talk we introduce the concept of "histotomography". For scalar problems with histogram data this holds the possibility of reconstruction with fewer rays. In vector and tensor problems it holds the promise of reconstruction of images that are in the null space of related integral transforms. We will illustrate with examples from scalar spectral attenuation tomography and tensor tomography methods for strain using neutrons, electrons and x-rays.

These notes correspond to a talk given in the Inverse Problems seminar series in the School of Mathematics, University of Manchester on March 8th 2018. A paper is in preparation with some numerical results with the current author and Dr Nick Polydorides from Edinburgh University.

1 Introduction

In conventional tomography we consider integrals along ray in direction ξ, ($|\xi| = 1$)

$$R(x,\xi) = \int_{-\infty}^{\infty} f(x+t\xi)\,dt$$

What if instead of the integral we knew the *distribution* or for discrete measurement to *histogram* along rays.

Put simply for each x, ξ and each y in the range of f the *measure* of the set of t values for which $f(x+t\xi) < y$ is the cumulative distribution $\Phi_{f,x,\xi}(y)$, and the distribution is $\phi_{f,x,\xi}(y) = \Phi'_{f,x,\xi}(y)$.

We define the scalar *histotomography transform*

$$Hf(x,\xi) = \phi_{f,x,\xi}$$

For a function of one variable f

$$\bar{f} = \int_{\mathbb{R}} y\phi_f(y)\,\mathrm{d}y = \int_{\Omega} f(x)\,\mathrm{d}x$$

is the integral (rather than the mean in probability distributions)

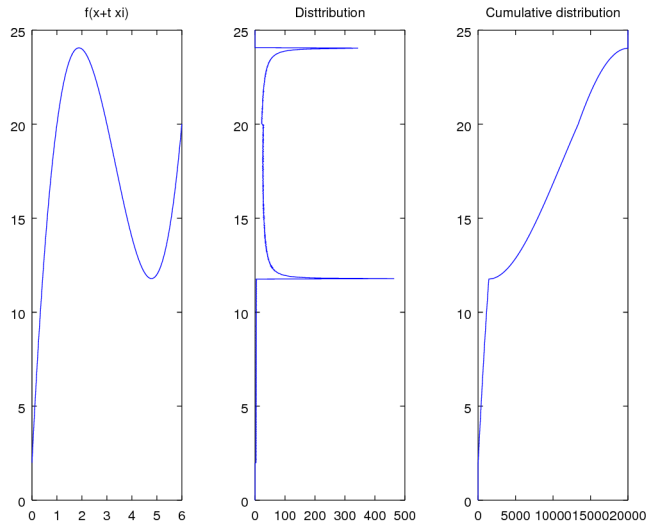

Figure 1: Illustration of distribution and cumulative distribution. The distributions are shown with the frequency on the horizontal axes for easy comparison with the graph of f.

We also define the k-th moment for $k \in \mathbb{N}$ as

$$m_k f = \int_{\mathbb{R}} y^k \phi_f(y)\,\mathrm{d}y = \int_{\Omega} f(x)^k\,\mathrm{d}x.$$

While the above is perhaps familiar for non-negative functions [3, Cor. A.1.] proves it for functions that can take negative values.

We recover the Radon transform from the first moment of the Histotomography transform

$$Rf(x,\xi) = \overline{Hf(x,\xi,\cdot)}.$$

We also have higher moments

$$m_k Hf((x,\xi,\cdot) = R(f^k)(x,\xi).$$

For the scalar case each of the moments produce no more data than the Radon transform and for a non-negative function exactly the same data!

A non-negative bounded function is determined completely by its moments [1] so the data are identical.

It is interesting to note however that while fitting a function f to its histotomography data Hf is a non-linear problem, each of the problems is linear

Consider the sub level set (ie inside a contour

$$Sf(y) := \{x \in \mathbb{R}^n | f(x) \leq y\}$$

Let $\chi_{Sf(y)}$ be the set that is 1 for $x \in Sf(y)$ and 0 elsewhere. Then

$$R\chi_{Sf(y)}(x,\xi) = \Phi_{f,x,\xi}(y)$$

so the cumulative distribution gives the Radon transform of the sub level set (or the histogram bin gives a 'fat' contour)

Example: In infra-red chemical species tomography (CST) [11, 2] suppose there is a species that absorbs strongly at one wavelength, and suppose that wavelength depends monotonically on frequency. The absorption spectrum then gives a histogram of the temperature along the line.

In CST it is widely thought that because they measure a function rather than a scalar along each line they should be able to do tomography with fewer projections.

What we know is that for a full set of projections we have the same data several times (each moment), and that with each bin of the histogram we essentially get a contour. But what about incomplete data?

We can can use limited angle or limited sensor results for each sublevel set. Microlocal reconstructions such as Λ-tomography [6] give the singular support – in our case for each histogram bin it would give the level set. Where some measurements are unavailable parts of level sets tangents to those directions are unavailable. But fitting a smooth functions to the contours *where we reliably have them* may give a better reconstruction With limited sensor size the two-step Hilbert transform method [12] reconstructs the area that is "fully illuminated". Some level sets might meet this criterion while others not.

2 Discrete tomography

- Algorithms such as DART [4] have been developed to for reconstructions where the range of the function is a finite set of values. In our case the characteristic function is 0 or 1.
- Geometric tomography results show that a *convex* body can be reconstructed from for projections from non rationally related angles [7]. If sub level sets are convex we can use this. Otherwise we get their convex hull.
- Another kind of discrete tomography is on graphs rather than Euclidean space. In this case the coloured graph tomography problem is a combinatorial version of histotomography[5].

3 Tensor ray transforms

Given a vector field v, and a second rank symmetric tensor field f we define the longitudinal ray transform (LRT) as

$$Iv(x,\xi) = \int_{-\infty}^{\infty} \xi \cdot v(x+t\xi)\,\mathrm{d}t$$

$$If(x,\xi) = \int_{-\infty}^{\infty} \xi \cdot f(x+t\xi)\cdot\xi\,\mathrm{d}t$$

for $x, \xi \in \mathbb{R}^n, \xi \neq 0$ where $\cdot$ denotes contraction. Similarly for rank k tensors.

The LRT has a null space consisting of *potential* tensor fields. In the case of vector fields this is just the usual definition, $f = \nabla u$ for a scalar u. Potential rank-2 tensor fields are those that can be expressed as $f = (\nabla u + \nabla u^T)/2$ for some vector field u.

In general, following [15], we define the operator d from rank-k to rank $k+1$ formed by differentiation and symmetrization. For $n \geq 2$ there is an explicit reconstruction for f from If of filtered back projection type, modulo this null space.

Let P_ξ be the projection of a symmetric second rank tensor field on to the plane perpendicular to ξ, then the transverse ray transform is defined as

$$Jf(x,\xi) = \int_{-\infty}^{\infty} P_\xi f(x+t\xi)\,\mathrm{d}t.$$

We consider the important case of dimension $n = 3$. For a direction $\eta \in \mathbb{R}^3$,

$$\eta \cdot Jf(x,xi) \cdot \eta = \int_{-\infty}^{\infty} \eta \cdot f(x+t\xi) \cdot \eta\,\mathrm{d}t$$

so in any plane normal to η this is simply the Radon transform of the component $\eta \cdot f \cdot \eta$. This means there is a simple reconstruction for six suitably chosen[10] directions η.

Both these problems have histotomography version, in which data is the distribution of $\xi \cdot f(x+t\xi) \cdot \xi$ or $P_\xi f(x+t\xi)$ respectively, along the ray $x + t\xi$.

In the case of the TRT with histogram data, one special case is that we have the distribution of $\eta \cdot f \cdot \eta$ along lines on a plane normal to η. As this is a Radon transform we have reduced to the scalar histotomography problem for this component on this plane.

This means we can use any of the limited data methods we have for the scalar histotomography problem

4 Doppler velocimetry

As Schuster [14] explains Doppler velocity tomography data is already understood as the distribution of velocity components along a line, in the direction of a line.

What we call the HLRT of the velocity field. The first moment is typically used and of course this gives only the solenoidal part of the velocity leaving the potential part to be determined by other means.

5 Potential part from the moment data

However consider the second moment which is the integral of $(v.\xi)^2$ along the line. Suppose the solenoidal part of v has already been recovered from the first moment and subtracted from the data, so without loss of generality $v = du$ for a scalar u. We notice the second moment is nothing but the LRT of the rank-2 tensor $du \odot du$, from [15] we know we can recover the Saint-Venant tensor, or equivalently the Kröner tensor [8]

$$K_{mn} = \epsilon_{mik}\epsilon_{nj\ell}\left(u_{,i}u_{,j}\right)_{k\ell} = \epsilon_{mik}\epsilon_{nj\ell}u_{,ik}u_{,j\ell}$$

where indices after commas denote differentiation

Consider now typical elements

$$K_{11} = u_{,23}^2 - u_{,22}u_{,33}$$

while

$$K_{12} = 2(u_{,12}u_{,33} - u_{,13}u_{,23})$$

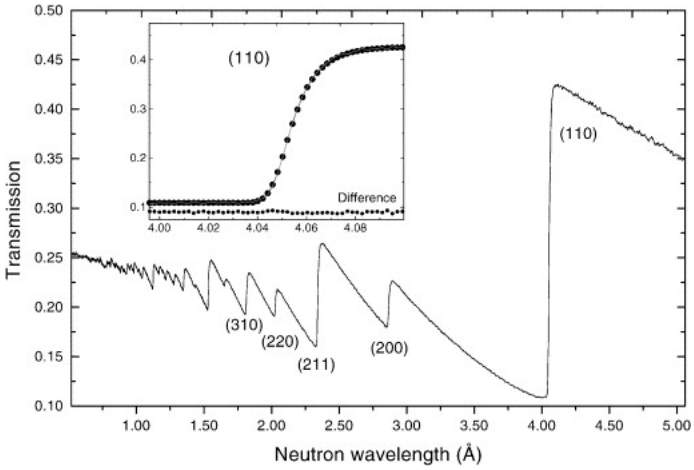

Figure 2: Neutron spectra from [13]

and the tensor K determines all the minors of the second derivative matrix $(d^2u)_{ij} = u_{,ij}$. Hence the adjugate matrix $\mathrm{Adj}d^2u$, and hence d^2u. In particular $\mathrm{trace}\, d^2u = \nabla^2 u$ is known and with Dirichlet boundary data for u, such as " u vanishes outside a compact set" we know u.

The LRT is interesting as occurs in Bragg edge neutron strain tomography. Linear strain is a symmetric derivative $\epsilon = du$ where u is the displacement vector field. This is in the null space of the LRT[10]. In practice this means the LRT data can only measure the change in the shape of the exterior of an object.

Of course one can use the finite element method to find u from this boundary data *if* the elastic modulus is known [16]. But can more data be extracted from neutron spectra?

6 Bragg edge spectra

Each crystolagraphic plane produces one "edge". When the crystal is strained in the direction of the neutron beam the edge will move proportionately. The LRT comes from the average shift of the mid point of the derivative of the spectrum.

Zooming in on one Bragg edge, which needs sufficient resolution of neutron wavelengths, reveals more detailed structure than simply a jump. The derivative of the spectrum gives the histogram LRT data up to a constant See fig reffig:braggshift.

Again from the histogram data we can deduce moments, and the k-th moment is the LRT of the symmetric powers $du \odot \cdots \odot du = du^{\odot k}$. These are not potential **but** they have a potential part. So we can recover the Saint Venant tensor of these. Unfortunately each is a non-linear partial differential equation for u. Solving for u is more work than using the FEM method mentioned above. However if the FEM method us used with assumed elastic moduli it is a way to check the solution is consistent with the full spectral data for each edge.

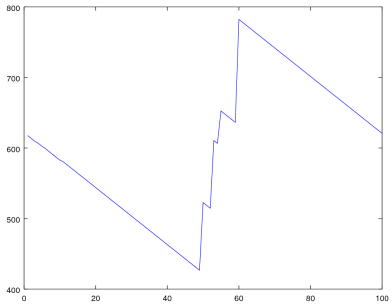

Figure 3: Shifted Bragg edges produce a saw tooth effect but the derivative is a histogram up to an added constant

7 Other spectral strain measurement techniques

In [10] we considered the case of monochromatic x-ray diffraction tomography of a polycrystaline material. The random orientation of the crystals means each crystalographic plane and mode produces a circular diffraction pattern. When a small gauge volume, still consisting of very many crystals, is strained this circle becomes an ellipse. As the diffraction patterns are summed over all the gauge volumes along the beam we have a superposition of concentric ellipses. As the diffraction pattern is measured only in teh plane we have a density function in two variables while the transverse competent of the strain tensor is given by three parameters. We see that we cannot deduce the distribution directly from this so we do not have the histogram transverse ray transform in this case.

Consider instead a single crystal with an incident narrow beam of monochromatic x-rays, electrons, or neutrons. This would normally produces a diffraction pattern consisting of small diffraction spots. To a good approximation the intensity is the square magnitude of the Fourier transform of the scatterers (eg nuclei or electron density) restricted to the plane. A displacement of the material along the beam will simply move the diffraction spots, application of a two by two matrix A will change the diffraction pattern by application of A^{-T} and scale the magnitude by $\det A$. In this case it seems we can deduce the histogram transverse ray transform from diffraction data provided the strained version of each spot is distinct. For a discussion of possible electron strain tomography see [9].

Acknowledgements

The author is supported by a Royal Society Wolfson Research Merit Award, and EPSRC grants EP/P02226X/1 EP/M022498/1 and EP/M010619/1.

References

[1] Naum Ilich Akhiezer. *The classical moment problem: and some related questions in analysis*, volume 5. Oliver & Boyd, 1965.

[2] Xinliang An, Thilo Kraetschmer, Kuya Takami, Scott T Sanders, Lin Ma, Weiwei Cai, Xuesong Li, Sukesh Roy, and James R Gord. Validation of temperature imaging by h_2o absorption spectroscopy using hyperspectral tomography in controlled experiments. *Applied optics*, 50(4):A29–A37, 2011.

[3] Fredrik Andersson. The doppler moment transform in doppler tomography. *Inverse problems*, 21(4):1249, 2005.

[4] Kees Joost Batenburg and Jan Sijbers. Dart: a practical reconstruction algorithm for discrete tomography. *IEEE Transactions on Image Processing*, 20(9):2542–2553, 2011.

[5] Cédric Bentz, Marie-Christine Costa, Dominique De Werra, Christophe Picouleau, and Bernard Ries. On a graph coloring problem arising from discrete tomography. *Networks*, 51(4):256–267, 2008.

[6] Adel Faridani, Erik L Ritman, and Kennan T Smith. Local tomography. *SIAM Journal on Applied Mathematics*, 52(2):459–484, 1992.

[7] R.J. Gardner. Chord functions of convex bodies. *J. London Math Soc*, 2(36):314–326, 1987.

[8] DV Georgievskii. Generalized compatibility equations for tensors of high ranks in multidimensional continuum mechanics. *Russian Journal of Mathematical Physics*, 23(4):475–483, 2016.

[9] Duncan N. Johnstone, Antonius T. J. van Helvoort, and Paul A. Midgley. Nanoscale strain tomography by scanning precession electron diffraction. *Microscopy and Microanalysis*, 23(S1):17101711, 2017.

[10] William RB Lionheart and Philip J Withers. Diffraction tomography of strain. *Inverse Problems*, 31(4):045005, 2015.

[11] Lin Ma, Weiwei Cai, Andrew W Caswell, Thilo Kraetschmer, Scott T Sanders, Sukesh Roy, and James R Gord. Tomographic imaging of temperature and chemical species based on hyperspectral absorption spectroscopy. *Optics express*, 17(10):8602–8613, 2009.

[12] Frederic Noo, Rolf Clackdoyle, and Jed D Pack. A two-step hilbert transform method for 2d image reconstruction. *Physics in Medicine & Biology*, 49(17):3903, 2004.

[13] Javier R Santisteban, Lyndon Edwards, Mike E Fitzpatrick, Axel Steuwer, Philip J Withers, Mark R Daymond, Michael W Johnson, Nigel Rhodes, and Erik M Schooneveld. Strain imaging by bragg edge neutron transmission. *Nuclear Instruments and Methods in Physics Research Section A: Accelerators, Spectrometers, Detectors and Associated Equipment*, 481(1-3):765–768, 2002.

[14] Thomas Schuster. 20 years of imaging in vector field tomography: a review. *Math. Methods in Biomedical Imaging and Intensity-Modulated Radiation Therapy (IMRT). Ser. Publications of the Scuola Normale Superiore*, 7:389, 2008.

[15] Vladimir Altafovich Sharafutdinov. *Integral geometry of tensor fields*, volume 1. Walter de Gruyter, 1994.

[16] CM Wensrich, JN Hendriks, A Gregg, MH Meylan, V Luzin, and AS Tremsin. Bragg-edge neutron transmission strain tomography for in situ loadings. *Nuclear Instruments and Methods in Physics Research Section B: Beam Interactions with Materials and Atoms*, 383:52–58, 2016.